EUROfusion

EUROFUSION CP(15)06/04

P. Frosi et al.

Structural Design of DEMO Divertor Cassette Body: FEM Analysys and Introductive Application of RCC–MRx Rules

12th International Symposium on Fusion Nuclear Technology (ISFNT)
Jeju Island, Korea
(14th September 2015 – 18th September 2015)

This work has been carried out within the framework of the EUROfusion Consortium and has received funding from the Euratom research and training programme 2014-2018 under grant agreement No 633053. The views and opinions expressed herein do not necessarily reflect those of the European Commission.

Structural design of DEMO Divertor Cassette Body: FEM analysis and introductive application of RCC-MRx design rules.

Paolo Frosi[a*], Giuseppe Mazzone[a], You Jeong-Ha[b]

[a]*Unità Tecnica Fusione- ENEA C.R. Frascati, Via E. Fermi 45, 00044 Frascati, Italy*
[b]*Max Planck Institute of Plasma Physics, Boltzmann Str.2, 85748 Garching, Germany*

This paper deals with the early steps in developing a structural fem model of DEMO Divertor. The study is focused on the thermal and structural analysis of the Cassette Body: a new geometry has been developed for this component: it is foreseen that the plasma facing component (PFC) will be directly placed on the cassette but for the Dome no choice has been adopted yet. For now the model contains only a suitable schematization of the Cassette Body and its objective is to analyze the effect produced by the main loads (electromagnetic loads, coolant pressure, thermal neutron and convective loads) on itself: an available estimate of loads is that one derived from ITER: for a proper translation some assumptions have been made and they are described in the paper. Now it is not a primary purpose to obtain some definitive statements about stresses, displacements, temperatures and so on; the authors want to construct a set of FEM models that will help all the decisions of DEMO Divertor design in its future development. This set is conceived as a tool that shall be improved to account for all the main enhancements that will be found in geometry, in material properties data and in load evaluations. Moreover, the main design variables (loads, material properties, some geometric items, mesh element size) are defined as parameters. This work considers also an introductive approach for future structural verification of the Divertor Cassette Body: so a concern of the Design and Construction Rules for Mechanical Components of Nuclear Installation (RCC-MRx) has been implemented. The FEM code used is Ansys rel. 15.

Keywords: fem, DEMO, Divertor, structural analysis, thermal analysis, RCC-MRx

1. Introduction

The DEMO project is a proposal for a nuclear fusion power plant that can be thought as an enhancement of ITER project along the way towards the commercial exploitation of nuclear fusion energy. The design takes advantage from the experience gained from the challenge related to ITER, but in spite of the acquired knowledge about physics, geometry of the machine, material behavior, prediction of loads and so on, other issues arise from this new design: because of its grater dimensions, its more demanding service conditions, the need of improving the actual technology and consolidating the safety in operations.

Within the several topics the tokamak design has been divided in, this paper debates about structural analysis needed to conceive the Cassette Divertor.

The Divertor main function is to withstand the plasma heat loads produced by the fusion process. So the Divertor has surely a thermal task, but also it must sustain the pressure due to the coolant fluid, the electromagnetic forces either in nominal or off-design conditions and so on.

Now only a new geometric concept of the Cassette Divertor is available derived from the general choices adopted by the Project Board. An analytical evaluation of the loads that reasonably will act on this component hasn't been prepared yet. As the aim of this work is the construction of an analysis tool that shall help the future designers' choices, at this time the load specifications haven't been regarded of critical influence: all data have been acquired from the ITER literature with the due adjustments as explained below.

Finally, a simplified approach related to the legal issues for nuclear installation (namely the French code RCC-MRx) has been engaged.

2. Geometry and fem model

The geometry of the Divertor has been fully revised: this is due either to the problems related to the blanket supports or to the remote handling needs. This new idea foresees that the plasma facing components will be directly connected on the cassette without hinges or trusses like in ITER. This should imply a simplification in the design and saving space. In Fig.1 there is a solid model of this new geometry: it has been developed within the EUROfusion tasks whose unpublished reference is EFDA_D_MHCL2. This paper deals only with the Cassette: the interface with the related components (inner, outer vertical target and the Dome) will be tackled when their new geometry will be available. The cassette contains at its interior several stiffening plates that must also guide the coolant water. In fig. 2 there is a transparent view that emphasizes this internal structure. In doing so, this revision of the cassette has a reduced volume and comparative analysis are in progress to judge about the suitability to insert the

*Corresponding author's email: paolo.frosi@enea.it

Dome. Now the volume is 0.718 m^3; the radial length is 3.35 m; and the toroidal width spans from 0.72 (inboard) to 1.08 m (outboard).

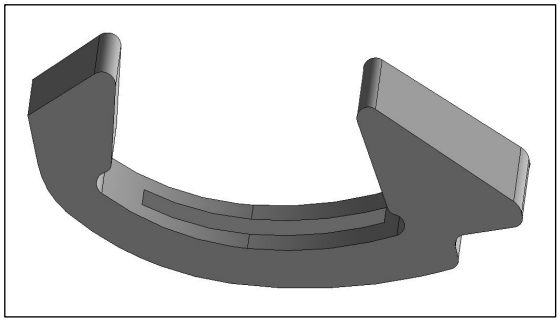

Fig. 1. CAD model of DEMO Divertor Cassette Body.

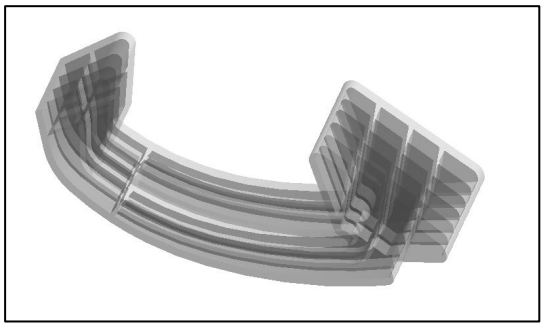

Fig. 2. Cassette's see-through image showing the ducts for cooling water.

This CAD model has been conceived in its global dimensions and almost all its geometric entities extend themselves along the whole component: so until now it hasn't been possible to consider small volumes in which to specialize the analysis: as a result the following mesh couldn't be mapped; for an overall and initial analysis it isn't a trouble, but this fact will be overcome in the future. In fig. 3 there is a plot of the mesh constructed inside the solid model: after some preliminary running a global size of 7 cm has been chosen as a trade-off between trust on results and quickness on execution.

Fig. 3. Finite element mesh for Divertor Cassette.

3. Eurofer material property and estimate of loads

An outstanding choice has regarded the adoption of Eurofer as a structural material. It is a Reduced Activation Ferritic Martensitic (RAFM 9% Cr steel) developed for fusion reactors in vessel components (this is the main reason for its choice). Therefore, a suitable water inlet temperature must be chosen either to guarantee an operational temperature higher than its ductile to brittle transition temperature (DBTT) or to protect against its high variation under irradiation (T_{min}>300-350 °C). Further, inlet water pressure must have the same order of magnitude of PWR (Pressurised Water Reactor), which allows a margin with regard to water saturation temperature. A disadvantage is due to the reduced creep strength, characteristic common to RAFM steels. T_{max}=550 °C is suggested as maximum temperature [1].

The material property adopted for the analysis have been taken from [2]. The adopted structural values are reported as a function of temperature in (tab.1): the Young modulus (E), the Poisson ratio (ν), the minimum yield strength at 0.2% ($R_{p0.2(min)}$), the minimum tensile strength ($R_{m(min)}$), and the maximum allowable stress (S_m).

Temp (°C)	E (MPa)	ν	$R_{p0.2(min)}$ (MPa)	$R_{m(min)}$ (MPa)	S_m (MPa)
20	217000	0.3	516	637	212
100	213000	0.3	480	595	212
200	207000	0.3	457	555	206
300	202000	0.3	442	517	192
400	196000	0.3	416	468	173

Tab. 1. Eurofer structural material properties.

The used thermal values are reported in tab.2: the specific heat capacity (C_p), the mass density (ρ), the thermal conductivity (λ), and the (secant) coefficient of thermal expansion (α).

Temp (°C)	C_p (J/kgK)	ρ (kg/m^3)	λ (W/mK)	α (10^{-6}/K)
20	442	7760	516	10.3
100	495	7740	480	10.7
200	538	7713	457	11.2
300	574	7685	442	11.6
400	623	7655	416	11.9

Tab. 2. Eurofer thermal material properties.

As a dedicated evaluation of load applied on the Divertor hasn't been available yet, some assumptions are needed to carry on the analysis. The considered loads are related to the normal operating conditions e.g. the neutron flux, the pressure and temperature of coolant, the convective cooling and to the normal operating incidents that is disruptions as reported below. The following statements affect the considered loads:

1) a surface heat load hasn't been considered because it acts on the PFCs and Dome that haven't been modeled:

2) the body heat load is only due to neutron flux whose order of magnitude has been chosen equal to 1W/cm^3 from internal technical discussions;

3) for the convective cooling a value of 20 kW/m^{2}K obtained from ordinary technical literature (forced convection of liquids) has been adopted;

4) the inlet water temperature has been chosen equal to 300 °C for the reasons mentioned beforehand:

5) the water pressure has been assumed to intake at 15 MPa.

The thoughts about structural loads begin from the concepts reported in the document EFDA_D_2MBSE3: the electromagnetic forces can be connected to the other plasma quantities with:

$$F \sim (I_p/a^2) * B_{tor} \quad (1)$$

where I_p is the plasma current, a is the plasma minor radius and B_{tor} is the toroidal magnetic field. This simple calculus used for some DEMO plasma options has been copied also for the same ITER values [3] to evaluate the coefficient that allows the comparison between the two cases as summarized in tab.3.

I_p (MA)	B_{tor} (T)	a^2 (m^2)	F	
14	6.8	5.1	1	DEMO
20.3	5.8	8.0	0.79	
15	5.3	4	1.07	ITER

Tab. 3. Correlation between ITER and DEMO for electromagnetic forces.

In doing so, before applying the ITER loads on DEMO Cassette Divertor, these values must be scaled according the factor 0.79/1.07=0.74 (the authors' reference now is I_p=20.3MA). All the values adopted are that one derived from the same document [3] and are summarized in tab. 4. The resultant forces (in radial, tangential and vertical directions) and the resultant moments (about to the Cassette Centroid and along the same directions) have been applied having been previously multiplied for the factor mentioned above.

	VDE-II	VDE-III	MD-I	MFD-II
F_{rad} (kN)	472	-800	-327	-199
F_{tan} (kN)	267	328	213	-28
F_{ver} (kN)	-407	-594	369	-403
M_{rad} (kNm)	-237	-282	-165	-31
M_{tan} (kNm)	-321	-545	-225	-123
M_{ver} (kNm)	-1402	-1690	-1122	-57

Tab. 4. Values of forces and moments derived from the equivalent ITER cases.

3. Plastic analysis

The whole study has been divided in two cases: the elastic analysis that has been used for the application of RCC-MRx code, and the elastic-plastic analysis that has been used for general structural considerations. The loads in "normal operational condition" (NOC), either thermal o structural have been analyzed acting together and separately. A multilinear isotropic hardening (MISO) temperature dependent material model available in ANSYS has been used and the values are taken from [2]. In the fig. 4 the average stress strain curve has been reported for clearness.

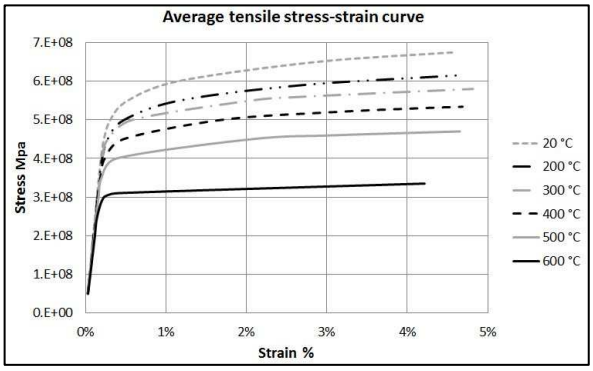

Fig. 4. Average tensile stress strain curve for some temperatures

The first step, preparatory for the two cases, is the thermal analysis. In fig. 5 there is a contour plot of the resulting temperature.

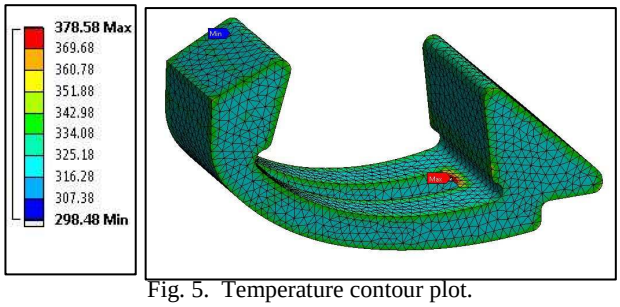

Fig. 5. Temperature contour plot.

For what concerns the supports of the Cassette on the vacuum vessel, because of the lack of information about geometric details and the local distribution of loads, only a general choice has been implemented: that is a frictionless support in the inboard region (simulating a simple bearing) and a composed (frictionless and cylindrical support) simulating a fixed constraint in the outboard region. This scheme allows radial expansions for thermal requirements.

In all the studied cases it can be written that there is a significant increase in stress in the region of the aforementioned constraint as reported in fig. 6 where it is plotted (as an example) the Von Mises stress related to applied water pressure and neutron flux.

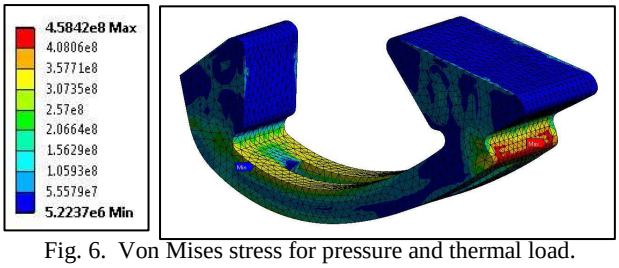

Fig. 6. Von Mises stress for pressure and thermal load.

According to the authors' interpretation, that region must react to a great percentage of applied loads: more the surface constrained ends at the edge of the Cassette

contributing to intensify the reaction stresses on the corner nodes that belong to a mesh that is not quite refined. This fact is confirmed by the plot of equivalent plastic strain reported in fig. 7. This fact is recurring in all cases.

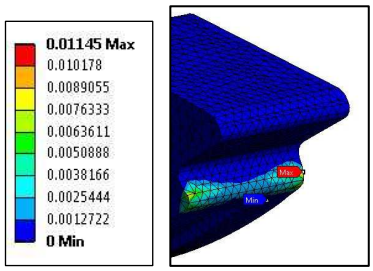

Fig. 7. Von Mises plastic strain for pressure and thermal load.

Therefore the role of attachments is relevant and their geometry shall be conceived carefully.

A further consideration, reported for heuristic purpose, is related to the pressure when it acts alone on the Cassette, it can be seen in fig. 8 that the equivalent stress is lower than the previous case and it has a different distribution: it signifies that, the thermal loads perform a great influence on structural and cinematic behavior of the structure.

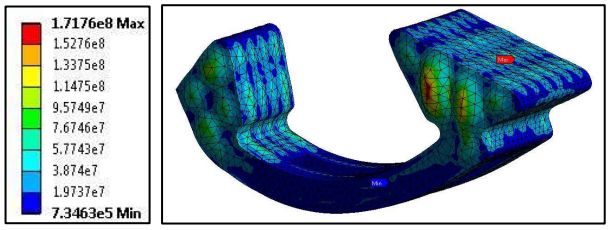

Fig. 8. Von Mises for pressure acting alone.

The cases related to the various disruption options mentioned above give information very uniform: the state of stress (not reported) exhibits a little increase in the maximum value compared to the previous ones and also the distribution is similar: this fact could be explained saying that the extrapolation of ITER results in the case of DEMO has been too much simplified: the resulting forces and moments have been applied to a geometry that is greater, ticker and stiffer than the ITER one and the resulting state of stress is much lower. A "customized" evaluation of magnetic loads seems to be required.

The last consideration worth to be explained is a result observed in the disruption's cases: the radial and tangential stress components exhibit their maximum and minimum values in the same region reported in fig. 7 (a sort of "butterfly distribution"): this behavior can be explained as a consequence of the moment values: from tab.4 it can be seen that the moment reaches its greatest values in the vertical direction and the high values of stress components in the plane normal to the vertical direction is a proof that bending loads are balanced by the fixed support as it should be in that region. In order to reduce this state of stress, lateral supports should be considered but in a way such that they avoid the irradiation streaming between cassettes.

4. Elastic analysis and RCC-MRx application

Another chapter of this work has regarded a preliminary evaluation of linearized stresses to respect the rules foreseen for nuclear installation. The same general considerations previously carried out can be said again. But because of the early stage of this analysis, some simplifications have been introduced.

The negligible creep temperature is 375 °C, and this is the case really considered even though the maximum temperature is 379 °C (fig.4). More because of the uncertainties and the lack of the data in irradiated conditions for Eurofer, the comparison has been performed only for standard conditions.

The line supporting segments chosen for the analysis have only an heuristic purpose: but the obtained results are meaningful anyway. In fig. 9 there is the positions of the two paths chosen.

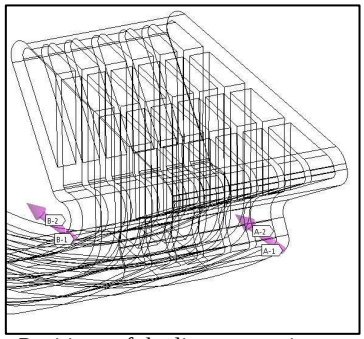

Fig. 9. Positions of the line supporting segments.

The path n.1 is the one on the right and it passes through the thickness in the aforementioned high stress region, the path n.2 is the other passing through the thickness in the upside surface. The case analyzed have regarded the application of:

1) primary and secondary loads that is water pressure, convective cooling and neutron heat generation in NOC:

2) secondary loads that is body neutron load and surface heat load given by convective cooling in NOC;

3) secondary loads that is thermal uniform temperature equal to the inlet water one (300 °C) in "stanby" conditions:

4) the difference between 2) and 3) for thermal stress range evaluation.

The case 1) can be connected to the result in fig. 6 and the same considerations can be assumed; the intensification of stress is even higher (in fig. 10 is reported the equivalent stress of this case): but even though this is related to only one node so it can be attributed to a rough (geometric and finite element) modeling of the attachments, this confirm the need of a proper design of these bearings.

The values related to the fig.10 (about 1000 MPa) are not reported because are meaningless, being really that region in the plastic regime.

The case 2) is equal to the result in fig. 8 because in this case the yield limit hasn't been overcome.

The case 3) behaves like case 1) confirming the great influence of thermal loads rather than pressure.

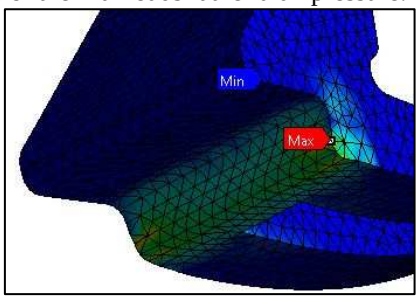

Fig. 10. Equivalent stress in NOC for primary and secondary loads.

The same elastic analysis has been performed when the disruption loads are superimposed to the NOC loads like reported in previous paragraph: but no further explanation seem necessary.

Finally the approach suggested by the RCC-MRx code must be illustrated. The simple analysis performed is related to prevent type P and type S damages in the case of Level A criteria.

To prevent type P damages the classical two relations for the two paths have been processed:

$$\overline{P_m} \le S_m(\vartheta_m) \tag{1}$$

$$\overline{P_m + P_b} \le 1.5 \cdot S_m(\theta_m) \tag{2}$$

where P_m is the general primary membrane stress intensity (octahedral shear theory), P_m+P_b is primary membrane plus bending stress intensity, S_m is the maximum allowable stress and θ_m is the mean temperature in the thickness for the loading considered.

With clear meaning of symbols (the values are in MPa), in the tab.5 there is a summary of the results obtained:

Path 1		θ_m=332.65°C	
P_m	2.04E7	S_m	1.86E8
P_m+P_b	4.46E7	1.5* S_m	2.79E8
Path 2		θ_m=326.55°C	
P_m	1.51E7	S_m	1.87E8
P_m+P_b	6.03E7	1.5* S_m	2.81E8

Tab. 5. Verification against type P damages.

To prevent type S damages the classical "3Sm" rule for the two paths has been assured:

$$Max\left(\overline{P_l + P_b}\right) + \overline{\Delta Q} \le 3 \cdot S_m \tag{3}$$

The values of the first term in (3) are obtained from the previous analysis and the values for the second term are obtained from the aforementioned case 4). With the same symbolism in tab.6 there are the relative results.

Path 1			
Max(P_m+P_b)+ΔQ	1.576E8	3* S_m	5.58E8
Path 2			
Max(P_m+P_b)+ΔQ	1.275E8	3* S_m	5.61E8

Tab. 6. Verification against type S damages.

At least in these two simple cases, the rule is verified.

Conclusions

An elastic and elastic-plastic finite element analysis has been performed for a preliminary geometry proposed for the DEMO Divertor Cassette. Even though the aim of this work has been to construct an overall numerical model that must be improved in the future, some conclusions can be deduced from this initial study. It is confirmed the relevant role played by the thermal loads; the geometry and the position of the attachment are significant and, finally, until suitable results for DEMO Divertor Cassette are unavailable, the same ITER quantities must be translated towards DEMO carefully.

Acknowledgments

This work has been carried out within the framework of the EUROfusion Consortium and has received funding from the Euratom research and training programme 2014-2018 under grant agreement No 633053. The views and opinions expressed herein do not necessarily reflect those of the European Commission."

References

[1] E. Visca, Manufacturing and testing of reference samples for the definition of acceptance criteria for the ITER divertor, Fusion Engineering and Design, vol. 85 (2010), pp. 1986-1991.

[2] RCC-MRx 2012 AFCEN Edition, Design and Construction Rules for Mechanical Components of Nuclear Installation.

[3] Iter Divertor Assessment Part 2, IDM UID HDVF5E